4. Reviewed in S. Inoué and E. D. Salmon, *Mol. Biol. Cell.* **6**, 1619 (1995).
5. D. H. Tippit, J. D. Pickett-Heaps, R. Leslie, *J. Cell Biol.* **86**, 402 (1980); T. J. Mitchison and M. W. Kirschner, *ibid.* **101**, 766 (1985); C. L. Rieder and S. P. Alexander, *ibid.* **110**, 81 (1990); J. H. Hayden, S. S. Bowser, C. L. Rieder, *ibid.* **111**, 1039 (1990); A. Merdes and J. De Mey, *Eur. J. Cell Biol.* **53**, 313 (1990); T. E. Holy and S. Leibler, *Proc. Natl. Acad. Sci. U.S.A.* **91**, 5682 (1994).
6. R. B. Nicklas and S. C. Ward, *J. Cell Biol.* **126**, 1241 (1994).
7. T. Mitchison and M. Kirschner, *Nature* **312**, 237 (1984).
8. R. B. Nicklas, *Chromosoma* **21**, 17 (1967).
9. G. Östergren, *Hereditas* **37**, 85 (1951).
10. Reviewed in R. B. Nicklas, *J. Cell Sci.* **89**, 283 (1988).
11. H. Bauer, R. Dietz, C. Röbbelen, *Chromosoma* **12**, 116 (1961).
12. M. F. Goodman, S. Creighton, L. B. Bloom, J. Petruska, *Crit. Rev. Biochem. Mol. Biol.* **28**, 83 (1993).
13. R. Dietz, *Chromosoma* **9**, 359 (1958).
14. R. B. Nicklas and C. A. Koch, *J. Cell Biol.* **43**, 40 (1969).
15. V. A. Lombillo, R. J. Stewart, J. R. McIntosh, *Nature* **373**, 161 (1995); V. A. Lombillo, C. Nislow, T. J. Yen, V. I. Gelfand, J. R. McIntosh, *J. Cell Biol.* **128**, 107 (1995); reviewed in A. Desai and T. J. Mitchison, *ibid.*, p. 1; A. A. Hyman, *Curr. Biol.* **5**, 483 (1995).
16. K. E. Sawin, K. LeGuellec, M. Philippe, T. J. Mitchison, *Nature* **359**, 540 (1992); D. W. Cleveland, *Trends Cell Biol.* **5**, 60 (1995).
17. S. Tugendrich, J. Tomkiel, W. Earnshaw, P. Hieter, *Cell* **81**, 261 (1995).
18. L. H. Hartwell and T. A. Weinert, *Science* **246**, 629 (1989).
19. H. G. Callan and P. A. Jacobs, *J. Genet.* **55**, 200 (1957).
20. R. E. Zirkle, *Radiat. Res.* **41**, 516 (1970).
21. C. L. Rieder, A. Schultz, R. Cole, G. Sluder, *J. Cell Biol.* **127**, 1301 (1994).
22. X. Li and R. B. Nicklas, *Nature* **373**, 630 (1995).
23. Budding yeast cells detect a single impaired chromosome, very likely because of improper spindle attachment [M. W. Neff and D. J. Burke, *Mol. Cell. Biol.* **12**, 3857 (1992); F. Spencer and P. Hieter, *Proc. Natl. Acad. Sci. U.S.A.* **89**, 8908 (1992); Y. Wang and D. J. Burke, *Mol. Cell. Biol.* **15**, 6838 (1995); F. Pangilinan and F. Spencer, *Mol. Biol. Cell* **7**, 1195 (1996); W. A. E. Wells and A. W. Murray, *J. Cell Biol.* **133**, 75 (1996)].
24. K. G. Hardwick, E. Weiss, F. C. Luca, M. Winey, A. W. Murray, *Science* **273**, 953 (1996).
25. S. Hughes-Schrader, *Biol. Bull.* **85**, 265 (1943).
26. J. G. Ault and C. L. Rieder, *Cell Motil. Cytoskeleton* **22**, 155 (1992).
27. C. L. Rieder, *Int. Rev. Cytol.* **79**, 1 (1982).
28. F. Schrader, *Chromosoma* **1**, 230 (1939); L. S. B. Goldstein, *Cell* **25**, 591 (1981).
29. Reviewed in B. John, *Meiosis* (Cambridge Univ. Press, Cambridge, 1990).
30. The hazards caused by pairing and recombination are unique to the first meiotic division, and the response, an exposed kinetochore, is also unique to that division. In the second meiotic division, the kinetochores are arranged just as in somatic mitosis: they are close to one another, they face precisely in opposite directions, and they are recessed in a pit (*29*).
31. J. R. McIntosh, *Cold Spring Harbor Symp. Quant. Biol.* **56**, 613 (1991).
32. C. L. Rieder, R. W. Cole, A. Khodjakov, G. Sluder, *J. Cell Biol.* **130**, 941 (1995).
33. G. J. Gorbsky and W. A. Ricketts, *ibid.* **122**, 1311 (1993).
34. R. B. Nicklas, S. C. Ward, G. J. Gorbsky, *ibid.* **130**, 929 (1995).
35. X. Li and R. B. Nicklas, *J. Cell Sci.*, in press.
36. J. Monod, J. P. Changeux, F. Jacob, *J. Mol. Biol.* **6**, 306 (1963). Alternatives such as antigen inaccessibility, loss, or redistribution caused by tension are unlikely (*34*).
37. G. J. Gorbsky, *Trends Cell Biol.* **5**, 143 (1995).
38. M. S. Campbell and G. J. Gorbsky, *J. Cell Biol.* **129**, 1195 (1995).
39. K. G. Hardwick and A. W. Murray, *ibid.* **131**, 709 (1995).
40. C. Connelly and P. Hieter, *Cell* **86**, 275 (1996).
41. R.-H. Chen, J. C. Waters, E. D. Salmon, A. W. Murray, *Science* **274**, 242 (1996).
42. Y. Li and R. Benezra, *ibid.*, p. 246.
43. M. Glotzer, *Curr. Biol.* **5**, 970 (1995).
44. R. W. King, P. K. Jackson, M. W. Kirschner, *Cell* **79**, 563 (1994); A. Murray, *ibid.* **81**, 149 (1995); A. Aristarkhov *et al.*, *Proc. Natl. Acad. Sci. U.S.A.* **93**, 4294 (1996).
45. Reviewed in D. E. Ingber *et al.*, *Int. Rev. Cytol.* **150**, 173 (1994); F. Lyall and A. J. El Haj, Eds, *Biomechanics and Cells* (Society for Experimental Biology/ Seminar Series 54, Cambridge Univ. Press, Cambridge, 1994); see also J. Howard and A. J. Hudspeth, *Neuron* **1**, 189 (1988); F. Sachs, *Mol. Cell. Biochem.* **104**, 57 (1991); A. J. Hudspeth and P. G. Gillespie, *Neuron* **12**, 1 (1994); C. I. Bargmann, *Cell* **78**, 729 (1994).
46. I thank D. Kubai for editorial review. Supported in part by grant GM-13745 from the Institute of General Medical Sciences, National Institutes of Health.

RESEARCH ARTICLE

Observation of Interference Between Two Bose Condensates

M. R. Andrews, C. G. Townsend, H.-J. Miesner, D. S. Durfee, D. M. Kurn, W. Ketterle

Interference between two freely expanding Bose-Einstein condensates has been observed. Two condensates separated by ~40 micrometers were created by evaporatively cooling sodium atoms in a double-well potential formed by magnetic and optical forces. High-contrast matter-wave interference fringes with a period of ~15 micrometers were observed after switching off the potential and letting the condensates expand for 40 milliseconds and overlap. This demonstrates that Bose condensed atoms are "laser-like"; that is, they are coherent and show long-range correlations. These results have direct implications for the atom laser and the Josephson effect for atoms.

The realization of Bose-Einstein condensation (BEC) in dilute atomic gases has created great interest in this new form of matter. One of its striking features is a macroscopic population of the quantum-mechanical ground state of the system at finite temperature. The Bose condensate is characterized by the absence of thermal excitation; its kinetic energy is solely the result of zero-point motion in the trapping potential (in general, modified by the repulsive interaction between atoms). This is the property that has been used to detect and study the Bose condensate in previous experiments. The Bose-Einstein phase transition was observed by the sudden appearance of a "peak" of ultracold atoms, either in images of ballistically expanding clouds (time-of-flight pictures) (*1*–*3*) or as a dense core inside the magnetic trap (*4*, *5*). The anisotropic expansion of the cloud (*1*–*3*) and the appearance of collective excitations at frequencies different from multiples of the trapping frequencies (*6*, *7*) were found to be in quantitative agreement with the predictions of the mean-field theory for a weakly interacting Bose gas (*8*–*11*). However, similar anisotropic expansion and excitation frequencies have been predicted for a dense classical gas in the hydrodynamic regime (*12*, *13*) and are therefore not distinctive features of BEC. Indeed, the nonlinear Schrödinger equation is equivalent to a hydrodynamic equation for superfluid flow, which, in many situations, is very similar to a classical hydrodynamic equation (*9*, *13*, *14*). Previous BEC studies have mainly concerned the "very cold" nature of the Bose condensate but have not revealed properties that directly reflect its coherent nature, such as its phase, order parameter (macroscopic wave function), or long-range order. In superconductors, the phase of the order parameter was directly observed through the Josephson effect, whereas in superfluid helium the observation of the motion of quantized vortices (*15*) provided indirect evidence.

The coherence of a Bose condensate has been the subject of many theoretical studies. Kagan and collaborators predicted that the Bose condensate will form first as a quasi-condensate consisting of very cold atoms but lacking long-range order, which is only established on a much longer time

The authors are in the Department of Physics and Research Laboratory of Electronics, Massachusetts Institute of Technology, Cambridge, MA 02139, USA.

scale (*16*). Stoof predicted that a coherent condensate would form immediately (*17*). Several groups discussed interference experiments and quantum tunneling for condensates (*18*–*29*). If the condensate is initially in a state of well-defined atom number, its order parameter, which is the macroscopic wave function, vanishes. However, the quantum measurement process should still lead to quantum interference and "create" the phase of the condensate (*20*, *23*–*25*, *27*, *28*), thus breaking the global gauge invariance that reflects particle number conservation (*30*). This is analogous to Anderson's famous gedanken experiment, testing whether two initially separated buckets of superfluid helium would show a fixed value of the relative phase—and therefore a Josephson current—once they are connected (*31*).

Arguments for and against such a fixed relative phase have been given (*31*, *32*). Even if this phase exists, there has been some doubt as to whether it can be directly measured, because it was predicted to be affected by collisions during ballistic expansion (*12*, *26*) or by phase diffusion resulting from the mean field of Bose condensed atoms (*21*, *25*, *27*, *33*). Additionally, the phase of the condensate plays a crucial role in discussions of an atom laser, a source of coherent matter waves (*34*–*37*).

The phase of a condensate is the argument of a complex number (the macroscopic wave function) and is not an observable. Only the relative phase between two condensates can be measured. Here, we report on the observation of high-contrast interference between two atomic Bose condensates, which is clear evidence for coherence in such systems.

The experimental setup. Two Bose condensates were produced using a modification of our previous setup (*3*, *7*). Sodium atoms were optically cooled and trapped and were then transferred into a double-well potential. The atoms were further cooled by radio frequency (rf)–induced evaporation (*38*). The condensates were confined in a cloverleaf magnetic trap (*3*), with the trapping potential determined by the axial curvature of the magnetic field $B'' = 94$ G cm^{-2}, the radial gradient $B' = 120$ G cm^{-1}, and the bias field $B_0 = 0.75$ G. The atom clouds were cigar-shaped, with the long axis horizontal. A double-well potential was created by focusing blue-detuned far-off-resonant laser light into the center of the magnetic trap, generating a repulsive optical dipole force. Because of the far detuning of the argon ion laser line at 514 nm relative to the sodium resonance at 589 nm, heating from spontaneous emission was negligible. This laser beam was focused into a light sheet with a cross section of 12 μm by 67 μm ($1/e^2$ radii), with its long axis perpendicular to the long axes of the condensates. The argon ion laser beam propagated nearly collinearly with the vertical probe beam. We aligned the light sheet by imaging the focused argon ion laser beam with the same camera used to image the condensates.

Evaporative cooling was extended well below the transition temperature to obtain condensates without a discernible normal fraction. Condensates containing 5×10^6 sodium atoms in the $F = 1, m_F = -1$ ground state were produced within 30 s. The presence of the laser-light sheet neither changed the number of condensed atoms from our previous work (*3*) nor required a modification of the evaporation path; hence, problems with heating encountered earlier with an optically plugged magnetic trap (*2*) were purely technical. In the present application, the argon ion laser beam was not needed to avoid a loss process, and thus we had complete freedom in the choice of laser power and focal parameters.

The double condensate was directly observed by nondestructive phase-contrast imaging (Fig. 1A). This technique is an extension of our previous work on dispersive imaging (*4*) and greatly improved the signal-to-noise ratio. The probe light frequency was far detuned from a resonant transition (1.77 GHz to the red), and thus absorption was negligible. Images were formed by photons scattered coherently in the forward direction. The phase modulation caused by the condensate was transformed into an intensity modulation at the camera by retarding the transmitted probe beam by a quarter-wave with a phase plate in the Fourier plane. Previously, the transmitted probe beam was blocked by a thin wire (dark-ground imaging).

Interference between the condensates was observed by simultaneously switching off the magnetic trap and the argon ion laser-light sheet. The two expanding condensates overlapped and were observed by absorption imaging. After 40 ms time-of-flight, an optical pumping beam transferred the atoms from the $F = 1$ hyperfine state to the $F = 2$ state. With a 10-μs delay, the atoms were exposed to a short (50 μs) circularly polarized probe beam resonant with the $F = 2 \rightarrow F' = 3$ transition and absorbed ~20 photons each. Under these conditions, the atoms moved ~5 μm horizontally during the exposure.

Absorption imaging usually integrates along the line of sight and therefore has only two-dimensional spatial resolution. Because the depth of field for 15-μm fringes is comparable to the size of an expanded cloud, and because the fringes are in general not parallel to the axis of the probe light, line-of-sight integration would cause considerable blurring. We avoided this problem and achieved three-dimensional resolution by restricting absorption of the probe light to a thin horizontal slice of the cloud. The optical pumping beam was focused into a light sheet of adjustable thickness (typically 100 μm) and a width of a few millimeters; this pumping beam propagated perpendicularly to the probe light and parallel to the long axis of the trap (*39*). As a result, the

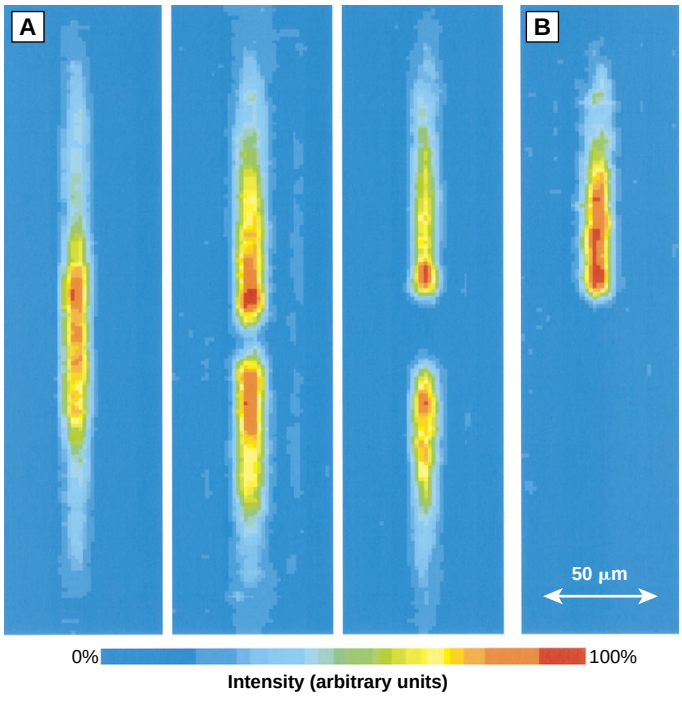

Fig. 1. (**A**) Phase-contrast images of a single Bose condensate (left) and double Bose condensates, taken in the trap. The distance between the two condensates was varied by changing the power of the argon ion laser-light sheet from 7 to 43 mW. (**B**) Phase-contrast image of an originally double condensate, with the lower condensate eliminated.

probe light was only absorbed by a thin slice of the cloud where the atoms were optically pumped. Because high spatial resolution was required from only the fraction of atoms residing in the slice, a good signal-to-noise ratio required condensates with millions of atoms.

Interference between two Bose condensates. In general, the pattern of interference fringes differs for continuous and pulsed sources. Two point-like monochromatic continuous sources would produce curved (hyperbolic) interference fringes. In contrast, two point-like pulsed sources show straight interference fringes; if d is the separation between two point-like condensates, then their relative speed at any point in space is d/t, where t is the delay between pulsing on the source (switching off the trap) and observation. The fringe period is the de Broglie wavelength λ associated with the relative motion of atoms with mass m,

$$\lambda = \frac{ht}{md} \qquad (1)$$

where h is Planck's constant. The amplitude and contrast of the interference pattern depends on the overlap between the two condensates.

The interference pattern of two condensates after 40 ms time-of-flight is shown in Fig. 2. A series of measurements with fringe spacings of ~15 μm showed a contrast varying between 20 and 40%. When the imaging system was calibrated with a standard optical test pattern, we found ~40% contrast at the same spatial frequency. Hence, the contrast of the atomic interference was between 50 and 100%. Because the condensates are much larger than the observed fringe spacing, they must have a high degree of spatial coherence.

We observed that the fringe period became smaller for larger powers of the argon ion laser-light sheet (Fig. 3A). Larger power increased the distance between the two condensates (Fig. 1A). From phase-contrast images, we determined the distance d between the density maxima of the two condensates versus argon ion laser power. The fringe period versus maxima separation (Fig. 3B) is in reasonable agreement with the prediction of Eq. 1, although this equation strictly applies only to two point sources. Wallis *et al.* (*26*) calculated the interference pattern for two extended condensates in a harmonic potential with a Gaussian barrier. They concluded that Eq. 1 remains valid for the central fringes if d is replaced by the geometric mean of the separation of the centers of mass and the distance between the density maxima of the two condensates. This prediction is also shown in Fig. 3B. The agreement is satisfactory given our experimental uncertainties in the determination of the maxima separations (~3 μm) and of the center-of-mass separations (~20%). We conclude that the numerical simulations for extended interacting condensates (*26*) are consistent with the observed fringe periods.

We performed a series of tests to support our interpretation of matter-wave interference. To demonstrate that the fringe pattern was caused by two condensates, we compared it with the pattern from a single condensate (this is equivalent to performing a double-slit experiment and covering one of the slits). One condensate was illuminated with a focused beam of weak resonant light 20 ms before release, causing it to disappear almost completely as a result of optical pumping to untrapped states and evaporation after heating by photon recoil (Fig. 1B). The resulting time-of-flight image did not exhibit interference, and the profile of a single expanded condensate matched one side of the profile of a double condensate (Fig. 4). The profile of a single expanded condensate showed some coarse structure, which most likely resulted from the nonparabolic shape of the confining potential. We found that the structure became more pronounced when the focus of the argon ion laser had some weak secondary intensity maxima. In addition, the interference between two condensates disappeared when the argon ion laser-light sheet was left on for

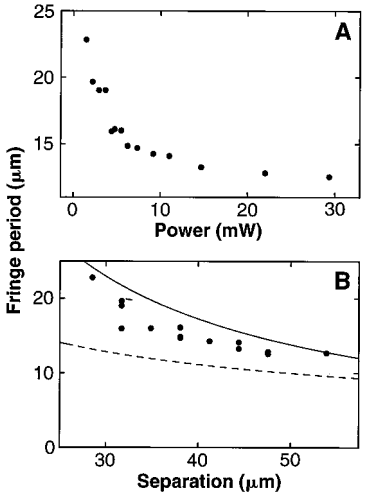

Fig. 3. (**A**) Fringe period versus power in the argon ion laser-light sheet. (**B**) Fringe period versus observed spacing between the density maxima of the two condensates. The solid line is the dependence given by Eq. 1, and the dashed line is the theoretical prediction of (*26*) incorporating a constant center-of-mass separation of 96 μm, neglecting the small variation (±10%) with laser power.

Fig. 2. Interference pattern of two expanding condensates observed after 40 ms time-of-flight, for two different powers of the argon ion laser-light sheet (raw-data images). The fringe periods were 20 and 15 μm, the powers were 3 and 5 mW, and the maximum absorptions were 90 and 50%, respectively, for the left and right images. The fields of view are 1.1 mm horizontally by 0.5 mm vertically. The horizontal widths are compressed fourfold, which enhances the effect of fringe curvature. For the determination of fringe spacing, the dark central fringe on the left was excluded.

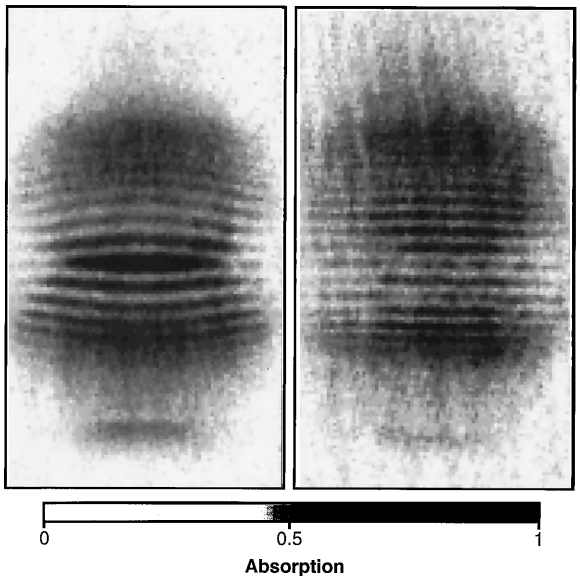

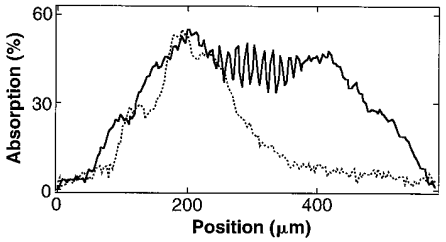

Fig. 4. Comparison between time-of-flight images for a single and double condensate, showing vertical profiles through time-of-flight pictures similar to Fig. 2. The solid line is a profile of two interfering condensates, and the dotted line is the profile of a single condensate, both released from the same double-well potential (argon ion laser power, 14 mW; fringe period, 13 μm; time of flight, 40 ms). The profiles were horizontally integrated over 450 μm. The dashed profile was multiplied by a factor of 1.5 to account for fewer atoms in the single condensate, most likely the result of loss during elimination of the second half.

2 ms after the magnetic trap was switched off. The absorption images showed that the two condensates were pushed apart and did not subsequently overlap.

Another test confirmed that the fringes were not attributable to density waves of two colliding condensates. Because the interference pattern depends on the phases of the condensates, the fringes should be sensitive to perturbations that strongly affect the phase but weakly affect the motion. Applying resonant rf radiation during the expansion of the two condensates caused a reduction of the fringe contrast by up to a factor of 4. The greatest reduction in contrast was found when the rf was swept 25 times between 0 and 300 kHz at 1 kHz. When a single condensate was exposed to the same rf radiation, no clearly discernible differences in the time-of-flight pictures were found. A possible explanation for the reduced fringe contrast is that frequent sweeps through the resonance in slightly inhomogeneous dc and rf magnetic fields created atoms in different superpositions of hyperfine states that only partially interfered.

The visibility of the fringes depended critically on several imaging parameters, as expected for the observation of such a finely striated structure. The fringes became almost invisible when the thickness of the optical pumping sheet was increased to 800 μm, whereas the focus of the imaging system could be varied over a wider range of up to ±1 mm without losing contrast. This implies that the fringes were at a small angle (~20 mrad) with respect to the probe beam.

The interference was remarkably robust. The fringes were very regular, although no attempt was made to control residual magnetic fields during the expansion. The high contrast implies that neither phase diffusion during expansion nor collisions with normal atoms were important. The latter aspect was studied in more detail when the rf evaporation was stopped at higher temperatures. We still observed fringes of identical contrast (*40*), but with decreasing amplitude because of the smaller number of condensed atoms. At the transition temperature, the fringes and the condensate disappeared.

We now consider whether the two condensates were truly independent. When the power of the argon ion laser was varied, we realized both well-separated and connected condensates. The chemical potential of the Bose condensates was ~4 kHz. The height of the barrier created by the argon ion laser was estimated to be ~2 kHz per milliwatt of power. At 100-mW laser power, the barrier height was 10 μK, resulting in a cloud that was already split well above the phase transition temperature of ~2 μK. The tunneling time of well-separated condensates was estimated to be greater than the age of the universe (*19*), and thus our experiment should be equivalent to Anderson's gedanken experiment ("What is the relative phase of two buckets of liquid helium?") (*31*) and also to an interference experiment between two independent lasers (*41*). Two independent condensates will show high-contrast interference fringes with a phase that varies between experiments (*20, 23, 24, 27*). In our experiment, however, even a fixed relative phase would have been detected as being random because of mechanical instabilities on a 10-μm scale. Once it becomes possible to distinguish between fixed and random phases, we should be able to investigate how phase coherence is established and lost. One possible experiment would be to adiabatically switch on the argon ion laser after condensation, thus splitting a single condensate, and to study how a definite phase becomes random as a function of time.

For argon ion laser powers below 4 mW, the interference pattern was slightly curved and symmetric about a central fringe that was always dark (Fig. 2). We conjecture that for small separations, the two condensates overlap very early during the expansion and interactions between them are not negligible. When the power of the laser-light sheet was lowered further, the number of fringes decreased, while the central dark feature persisted and eventually lost contrast. For such low powers we were in the regime where the condensates were not fully separated.

The observation of matter-wave interference with a 15-μm period required sources of atoms with a matter wavelength of 30 μm, corresponding to a kinetic energy of 0.5 nK or 1/2600th of the single-photon recoil energy. This energy is much smaller than the mean-field energy of Bose condensates in our trap (~100 nK) and also much less than the zero-point energy (~15 nK). Fortunately, the extremely anisotropic expansion of the condensates released from the cloverleaf trap yields atoms with very long de Broglie wavelengths in the axial direction.

Outlook. The techniques of condensate cutting and three-dimensional absorption imaging described above open up possibilities for further investigations. We have switched off the trap and observed the existence of the relative phase of two condensates. The next logical step is to combine this technique with our recently demonstrated output coupler for a Bose condensate (*42*). In that case, recording the interference pattern for the first output pulse creates a coherent state of the trapped condensate through the quantum measurement process. Subsequent output pulses could be used to study the time evolution of the phase and the loss of coherence resulting from phase diffusion (*21, 27, 33*).

By using a thinner barrier (~1 μm) between the two condensates, it should be possible to reliably establish a weak link and study quantum tunneling, or the Josephson effect, for atoms (*18, 19, 29*). For superconductors, the Josephson effect is the usual way of detecting the phase of the order parameter. For atomic Bose condensates, we observed a relative phase directly. This is an example of the complementary physics that can be explored with Bose condensation in dilute atomic gases. Moreover, we have shown the technical feasibility of manipulating magnetically trapped Bose condensates with far-off-resonant laser beams. Hence, it is possible to perform "microsurgery" of Bose condensates, such as shaping the trapping potential or creating localized excitations (for example, using such a laser beam as a "paddle wheel" to excite rotational motion).

The observation of high-contrast interference fringes is clear evidence for spatial coherence over the extent of the condensates (*43*). In theoretical treatments, coherence (off-diagonal long-range order) has been used as the defining criterion for BEC (*30*). Our results also demonstrate that a Bose condensate consists of "laser-like" atoms, or atoms that interfere without any further selection by collimating apertures. This opens up the field of coherent atomic beams. Our recent work on an output coupler for a Bose condensate (*42*) already contained all the elements of an atom laser (*44*), because it created multiple pulses that should have a coherence length exceeding the size of a single condensate. Although this has been described as the first realization of an atom laser (*45*), we felt the demonstration that Bose condensed atoms have a measurable phase was a crucial missing feature. The present work addresses this issue and demonstrates that a Bose condensate with an output coupler is an atom laser.

Note added in proof: We have recently combined the rf output coupler (*42*) with the observation of interference between two condensates. The output pulse from a split condensate showed high-contrast interference that was very similar to the results discussed above (*46*). This proves that the rf output coupler preserves the coherence of the condensates.

REFERENCES AND NOTES

1. M. H. Anderson, J. R. Ensher, M. R. Matthews, C. E. Wieman, E. A. Cornell, *Science* **269**, 198 (1995).
2. K. B. Davis *et al.*, *Phys. Rev. Lett.* **75**, 3969 (1995).
3. M.-O. Mewes *et al.*, *ibid.* **77**, 416 (1996).
4. M. R. Andrews *et al.*, *Science* **273**, 84 (1996).
5. C. C. Bradley, C. A. Sackett, R. G. Hulet, in preparation; see also C. C. Bradley *et al.*, *Phys. Rev. Lett.* **75**, 1687 (1995).

6. D. S. Jin, J. R. Ensher, M. R. Matthews, C. E. Wieman, E. A. Cornell, *Phys. Rev. Lett.* **77**, 420 (1996).
7. M.-O. Mewes *et al.*, *ibid.*, p. 988.
8. M. Edwards, P. A. Ruprecht, K. Burnett, R. J. Dodd, C. W. Clark, *ibid.*, p. 1671.
9. S. Stringari, *ibid.*, p. 2350.
10. M. Holland and J. Cooper, *Phys. Rev. A* **53**, R1954 (1996).
11. Y. Castin and R. Dum, *Phys. Rev. Lett.* **77**, 5315 (1996).
12. Y. Kagan, E. L. Surkov, G. V. Shlyapnikov, *Phys. Rev. A* **54**, R1753 (1996).
13. A. Griffin, W.-C. Wu, S. Stringari, in preparation.
14. P. Nozières and D. Pines, *The Theory of Quantum Liquids* (Addison-Wesley, Reading, MA, 1990), vol. 2.
15. P. W. Anderson, *Rev. Mod. Phys.* **38**, 298 (1966).
16. Y. Kagan, in *Bose-Einstein Condensation*, A. Griffin, D. Snoke, S. Stringari, Eds. (Cambridge Univ. Press, Cambridge, 1995), pp. 202–225.
17. H. T. C. Stoof, *ibid.*, pp. 226–245.
18. J. Javanainen, *Phys. Rev. Lett.* **57**, 3164 (1986).
19. F. Dalfovo, L. Pitaevskii, S. Stringari, *Phys. Rev. A* **54**, 4213 (1996).
20. J. Javanainen and S. M. Yoo, *Phys. Rev. Lett.* **76**, 161 (1996).
21. E. M. Wright, D. F. Walls, J. C. Garrison, *ibid.* **77**, 2158 (1996).
22. W. Hoston and L. You, *Phys. Rev. A* **53**, 4254 (1996).
23. M. Naraschewski, H. Wallis, A. Schenzle, J. I. Cirac, *ibid.* **54**, 2185 (1996).
24. J. I. Cirac, C. W. Gardiner, M. Naraschewski, P. Zoller, *ibid.*, p. R3714.
25. T. Wong, M. J. Collett, D. F. Walls, *ibid.*, p. R3718.
26. H. Wallis, A. Röhrl, M. Naraschewski, A. Schenzle, *ibid.*, in press.
27. Y. Castin and J. Dalibard, in preparation.
28. E. M. Wright, T. Wong, M. J. Collett, S. M. Tan, D. F. Walls, in preparation.
29. M. W. Jack, M. J. Collett, D. F. Walls, *Phys. Rev. A* **54**, R4625 (1996).
30. K. Huang, *Statistical Mechanics* (Wiley, New York, ed. 2, 1987).
31. P. W. Anderson, in *The Lesson of Quantum Theory*, J. D. Boer, E. Dal, O. Ulfbeck, Eds. (Elsevier, Amsterdam, 1986), pp. 23–33.
32. A. J. Leggett and F. Sols, *Found. Physics* **21**, 353 (1991).
33. M. Lewenstein and L. You, *Phys. Rev. Lett.* **77**, 3489 (1996).
34. C. J. Bordé, *Phys. Lett. A* **204**, 217 (1995).
35. R. J. C. Spreeuw, T. Pfau, U. Janicke, M. Wilkens, *Europhys. Lett.* **32**, 469 (1996).
36. M. Holland, K. Burnett, C. Gardiner, J. I. Cirac, P. Zoller, *Phys. Rev. A* **54**, R1757 (1996).
37. M. Olshanii, Y. Castin, J. Dalibard, in *Laser Spectroscopy XII*, M. Ignuscio, M. Allegrini, A. Sasso, Eds. (World Scientific, Singapore, 1996), pp. 7–12.
38. W. Ketterle and N. J. van Druten, in *Advances in Atomic, Molecular, and Optical Physics*, B. Bederson and H. Walther, Eds. (Academic Press, San Diego, CA, 1996), vol. 37, pp. 181–236, and references therein.
39. Inhomogeneities in the pumping sheet caused weak striations that were perpendicular to the observed fringes and could therefore be clearly distinguished.
40. The thermal cloud had expanded so much that it contributed negligible background.
41. R. L. Pfleegor and L. Mandel, *Phys. Rev.* **159**, 1084 (1967).
42. M.-O. Mewes *et al.*, *Phys. Rev. Lett.* **78**, 582 (1997).
43. We are not distinguishing here between different aspects of coherence that are expressed by expectation values of products of one, two, or four field operators.
44. E. Cornell, *J. Res. Natl. Inst. Stand. Technol.* **101**, 419 (1996).
45. K. Burnett, *Physics World*, 18 (October 1996).
46. In these experiments, we transferred ~50% of the atoms into the $F = 1$, $m_F = 0$ state, immediately turned off the argon ion laser-light sheet to allow the two out-coupled condensates to overlap, and switched off the magnetic trap 2 ms later to avoid acceleration by quadratic Zeeman shifts.

47. We thank M. Naraschewski and H. Wallis for enlightening discussions; their theoretical simulations (*26*) were helpful in selecting the final parameters for the experiment. We also thank M.-O. Mewes for essential contributions during the early phase of the experiment, S. Inouye for experimental assistance, and D. Kleppner and D. Pritchard for valuable discussions. Supported by the Office of Naval Research, NSF, Joint Services Electronics Program, and the Packard Foundation. D.M.K. was supported by a NSF Graduate Research Fellowship, C.G.T. by a North Atlantic Treaty Organization (NATO) Science Fellowship, and H.-J.M. by Deutscher Akademischer Austauschdienst (NATO Science Fellowship).

11 December 1996; accepted 19 December 1996